Preparation and cytological study
of collagen/nano-hydroxyapatite/graphene oxide composites

JIANHUA WANG[1, 3]*, YINGYING WANG[1], DESHUAI LIU[1], QIU YANG[1],
CHENGUANG HUANG[1], CHUNRONG YANG[2], QIQING ZHANG[1]

[1] Institute of Biomedical and Pharmaceutical Technology, Fuzhou University, Fuzhou, China.
[2] Department of Materials Science and Engineering, Fujian University of Technology, Fuzhou, China.
[3] Bote Biotech. Co., Ltd. Fujian, China.

Purpose: Biomimetic mineralized composite scaffolds are widely used as natural bone substitute materials in tissue engineering by inducing and assembling bonelike apatite. In this study, the single lamellar structure of graphene oxide (GO) powder was prepared via an improved Hummers' method. *Methods:* To better mimic natural bone, the collagen (COL)/Nano-hydroxyapatite (*n*HA)/graphene oxide (GO) composite material was prepared by simulated body fluid (SBF) method using COL/GO as a matrix template. Hydroxyapatite (HA) with calcium ion deficiency was achieved via biomimetic mineralization, and it had properties closer to those of natural bone than pure HA has. *Results:* The mineralized COL/*n*HA/GO composites exhibited loose porous structures, and the connectivity of the holes was good and thus beneficial to the exchange of nutrients and excreted metabolites. *Conculsions:* Antibacterial and MTT experiment confirmed that the COL/*n*HA/GO composite material had excellent antibacterial property and biocompatibility. Hence, these results strongly suggested the mineralized COL/*n*HA/GO composite is a good candidate biomaterial to be applied in bone tissue engineering.

Key words: nano-hydroxyapatite, graphene oxide, biomimetic mineralization, collagen

1. Introduction

Bone defects have become a serious and significant health concern, and the treatment of bone defects is still clinically challenging in the orthopedics. Bone tissue engineering shows a great potential for the repair of bone defects. Although many single or composite artificial materials have been employed for the treatment of bone repair in the past several decades, the mechanical strength, which is one of the most critical problems and concerns for bone substitutes, still needs to be improved [15], [1], [21]. Particularly, an ideal scaffold should not only have excellent biocompatibility and biodegradability, it should also have mechanical properties that approximate the composition and structure of natural bone [19], [10]. Recently, biomimetic mineralization is an important research direction in the field of biomimetic materials. Such research mainly involve the study of minerals in living organism in order to synthesize mineral materials with similar structures and properties with natural biological tissues by imitating the process of the mineralization of organism [12], [26]. Simulating the composition and structure of natural bone and using biomimetic mineralization *in situ* method of preparation of bone substitutes have become a research hotspot.

In relation to that, COL has been widely used in bone tissue engineering due to its excellent biocompatibility, negligible immunogenicity, cell adhesion, and biodegradability. COL can also specifically interact with growth factors which promote cell ingrowth and remodeling [27], [32]. However, COL use is commonly limited by its weak mechanical properties and high release rate [29], [5], [30].

On the contrary, GO, a derivative of graphene functionalization, have gained much interest because of its great biocompatibility, bacteriostasis and non-

toxicity [9], [16], [22], [20]. More importantly, GO possesses a high mechanical strength [23]. It is also noteworthy that the GO composite scaffold was reported to show significant increase in Young's modulus and enhanced proliferation and adhesion of mesenchymal stem cells (MSCs) [6], [13], [14]. Therefore, it can be stated that the GO composite scaffold is a promising material for bone replacement.

On the other hand, HA is the main inorganic mineral component of teeth and bones. Due to its outstanding bioactivity and biocompatibility, it has been widely used as bone cavity filling, metallic implant coating and bone graft substitute [2], [3], [11], [24], [25]. Previous research showed that nHA promoted the adhesion and proliferation of osteoblasts cultured *in vitro*. However, the disadvantages of HA, such as brittleness and toughness, limit its application in the field of bone repair [18]. To prepare ideal scaffolds, natural organic matter/HA mineral materials were achieved by controlling the HA biomineralization process and based on natural organic matter macromolecule materials [17]. The simulated humoral method is a type of biomimetic mineralization approach. By simulating the mineralization mechanism of nHA, the apatite layer is naturally deposited in the fluid similar to human tissue.

In this article, the single lamellar structure of GO powder was prepared via an improved Hummers' method and the COL/nHA/GO composites were synthesized by biomimetic mineralization method. The physical and chemical properties and biocompatibility of GO powder and COL/nHA/GO composites were investigated. Finally, we confirmed that the scaffolds were able to provide suitable environment for cell proliferation and adhesion in favor of orthopedic defect reconstruction and to serve as a promising candidate for bone tissue engineering.

2. Materials and methods

Materials

Bovine COL was supplied by Bote Biotech, Co., Ltd. (Fuzhou, China). GO was fabricated according to Hummers' method [7], with some modification. Dulbecco's Modified Eagle Medium/Nutrient Mixture F-12 (DMEM/F-12), foetal bovine serum (FBS), penicillin and streptomycin were bought from Bioman Biotechnology Co., Ltd. (Fuzhou, China). 3-(4,5--Dimethylthiazol-2-yl)-2,5-diphenyl-tetrazo-liumbromile (MTT) was purchased from the Bio Sharp Co. (USA).

Preparation of GO

GO was fabricated according to Hummers' method, with some modification. Firstly, concentrated H_2SO_4 (108 mL) and H_3PO_4 (12 mL) were added into a 500 ml three-mouth flask and ice bathed for 10 min. Then, graphite powder (5 g) and the $NaNO_3$ (2.5 g) were added under a strong agitation. The $KMnO_4$ (15.0 g) was divided and slowly added into the above mentioned mixture, and the temperature was controlled not to exceed 5 °C. The mixture was stirred in ice bath for 3 h, and then stirred in a water bath of 40 °C for 1 h. The mixture was heated up rapidly to 98 °C for 60 mins and the deionized water was added continually until the mixture reached 400 ml. After 5 min, H_2O_2 (15 mL) was added to remove the excess oxidant, followed by repeated washing with super pure water and 5% HCl solution untill no sulfate ion was found in the solution. Lastly, the reaction products were freeze-dried to obtain the single lamellar structure of GO powder.

Preparation of COL/GO composites

The GO aqueous solution (6 mg/L) was mixed with the COL solution (0.6 wt. %) to obtain a COL/GO solution. The mass fraction of GO was 0, 1, and 4 wt. %. COL/GO composite porous scaffolds were obtained after thorough mixing and freeze-drying. The freeze-dried scaffolds were immersed in a crosslinking solution containing 0.2 mol/L of ribose, 10% acetone, and 2% ammonia water at room temperature. After reaction at room temperature for 24 h, the scaffolds were washed every 3 h for at least five times and freeze dried again.

Preparation of simulated body fluids (SBF)

The 1.5×SBF solution preparation method is shown in Table 1. COL/GO biocomposites were prepared via in vitro biomimetic mineralization in 1.5 times SBF (1.5×SBF). The reagent was gradually added during

Table 1. 1.5×SBF Solution (1000 mL)

Order	Reagent	Addition
0	Ultrapure water	750 mL
1	NaCl	11.994 g
2	$NaHCO_3$	0.525 g
3	KCl	0.336 g
4	$K_2HPO_4 \cdot 3H_2O$	0.342 g
5	$M gCl_2 \cdot 6H_2O$	0.458 g
6	1 kmol/m^3 HCl	60 mL
7	$CaCl_2$	0.417 g
8	Na_2SO_4	0.107 g
9	$(CH_2OH)_3CNH_2$	9.086 g

magnetic stirring to prepare the simulated fluid. The prepared SBF was stored in plastic bottles, sealed, and placed in a refrigerator at 5–10 °C.

Biomimetic mineralization with COL-based nHA/GO composites

The cross-linked COL/GO composite was irradiated with gamma rays, immersed in 1.5×SBF solution under sterile conditions, and placed in a low-speed rolling bed for mineralization at 37 °C constant temperature. After mineralization for 3 days (change in liquid every 24 h), the samples were taken out, washed with distilled water, and freeze dried to remove moisture.

Characterization of GO

X-ray diffraction (XRD) and Fourier transform infrared spectroscopy (FTIR, Spectrum BX, Perkin Elmer, Waltham, MA) were used to characterize the structure of GO powder. The FTIR uses a diffuse reflection mode and scanning range of 4000–500 cm^{-1}.

The morphology of GO powder was characterized by environmental scanning electron microscopy (SEM, Philips-FEI XL30 ESEM-TMP, Eindhoven, Netherlands), and the morphology of the sample was observed after metal spraying for 5 min.

Thermogravimetric analysis (TG) was used to test the loss of GO weight at high temperature in order to measure the thermal stability of GO.

Characterization of mineralized COL/nHA/GO composite

The internal microstructure of the mineralized COL/nHA/GO composite materials and the effect of mineralization were observed through SEM. Energy dispersive X-ray spectroscopy (EDX) and X-ray photoelectron spectroscopy (XPS) were used to detect the change of element atomic. It further verified the presence of HA deposition in the mineralized composite material. XRD was used to characterize the composition of matter and crystal structure. By analyzing its diffraction pattern, the composition of mineralized composite materials was obtained.

Bacteriostatic test of mineralized COL/nHA/GO composite

The beef paste (10 g), NaCl (5 g), AGAR (15–20 g) and water (1000 mL) were added in the beaker. The content was heated and stirred constantly until the AGAR culture medium dissolved. The hot medium was poured into the triangle, then in 121 high pressure sterilization for 30 min. The cool sterilization culture medium was poured into the sterilized Petri dish. The *Staphylococcus aureus* was isolated in the sterile water and the spores were dispersed for several minutes. Finally, 10^5 cFU/mL *Staphylococcus aureus* suspensions were prepared. A certain concentration of mixed spore suspension (0.5 mL) was injected into the Petri dishes with a syringe and the culture medium was coated evenly. The circular sheet COL/nHA/GO composite material was adhered to the surface of the culture medium and was cultured in the incubator. The presence of bacteriostatic ring was observed around the material after 24 h.

Isolation and culture of osteoblasts

Osteoblasts were isolated from the 2-d-old SD rats of clean grade under sterile condition and purified by differential centrifugation technique for several times. All the procedures were approved by Medical University of Fujian Institutional Animal Care and Use Committee. Osteoblasts were collected into a 25 cm^2 culture flask and cultured in DMEM/F-12 supplemented with FBS (10%) at 37 °C with 5% (v/v) carbon dioxide (CO$_2$). The medium was changed every 2 days and the passage 3–4 cells were used for follow-up experiments.

Cell viability and proliferation

Cell viability was assessed by AO/EB double staining. Osteoblasts suspension (1×10^5) cells/ml were cultured using the leach liquor of COL/nHA/GO composite material in 48-well plate and then respectively incubated for 3, 5 and 7 days. The plates were washed with PBS for three times. A mixture of AO (100 μg/mL) and EB (100 μg/mL) was then added under dark environment for 10-min staining, followed by washing with PBS. Finally, the pictures of strained cells were observed under an inverted fluorescence microscope (Olympus, IX71, Tokyo, Japan).

The number of viable cells attached on the COL/nHA/GO composite material was assessed by MTT staining [28]. Osteoblasts suspension (1×10^5) cells/mL were cultured using the leach liquor of COL/nHA/GO composite material in 96-well plate. Then, 20 μL MTT solution (5 mg/mL in PBS) was added to each well at different culture time points (7 days) and incubated at 37 °C with 5% (v/v) CO$_2$ for 4 h. Then, the DMSO (200 μL) was added to the top of each well to dissolve the formazan crystals. The absorbances of liquid in each well were measured at 490 nm using an enzyme-linked immunosorbent assay reader (DNM-9602, Beijing Perlong New Technology Co., Ltd., China).

All the original data were presented as the mean and standard deviation, in the research field, based on which to make the quantitative analysis. The statistical significance of the data were performed using analysis of variance. $P < 0.05$ was considered statistically significant and $p < 0.01$ was considered to be highly significant.

3. Results

3.1. Characterization of prepared GO

SEM

As shown in Fig. 1A, the translucent multilayer sheets of graphite were stacked and a rough surface with wrinkles was observed. Compared with graphite, the prepared GO (Fig. 1B) had a distinct outline and had a smooth and transparent surface, with few layers and wrinkles at the edges. The morphology of graphite and GO is different because there are few oxygen-containing groups in graphite, and the layer are easy to reunite under the effect of van der Waals force. In the process of GO preparation, edge layer introduces a large number of reactive oxygen, which increases the lamellar spacing and greatly reduces the acting force between layers. After the ultrasonic peeling, the single-layer structure is presented.

XRD

The XRD spectrogram of GO is shown in Fig. 2A. The characteristic peak of GO appeared at 11.38 and there were no other impurity peak. The distance between the layers was calculated by the following formula:

$$2d \sin \theta = n\lambda \tag{1}$$

The λ is the wavelength of the X ray, the θ is the diffraction angle, the d is the spacing of the planes, and n is the diffraction series. Calculation results of d (0.783 nm) indicates that the oxygen GO has been separated by ultrasound to get a larger interval. The results also indicate that the GO with fewer layers can be produced by this method.

FTIR spectroscopy

GO exhibited major characteristic bands at 3407 cm^{-1}, 1625 cm^{-1} and 1041 cm^{-1} in Fig. 2(B), which are corresponding to the stretching vibration of –OH, carboxyl and epoxy. Graphite powder has a relatively small peak near 3400 cm^{-1}, which is attributed to the -OH stretching vibration of water molecules. The vibration at 1380 cm^{-1} is a carboxyl c-o vibration, and in 1221 cm^{-1} is a stretching vibration of c-o-c on the GO surface. Due to the strong hygroscopicity of the GO sample, the absorption peak of carboxyl or water molecule was strongest at 1625 cm^{-1}. The presence of oxygen groups above indicates that the graphite has been oxidized. These polar groups, especially the presence of hydroxyl groups, make it easy for GO
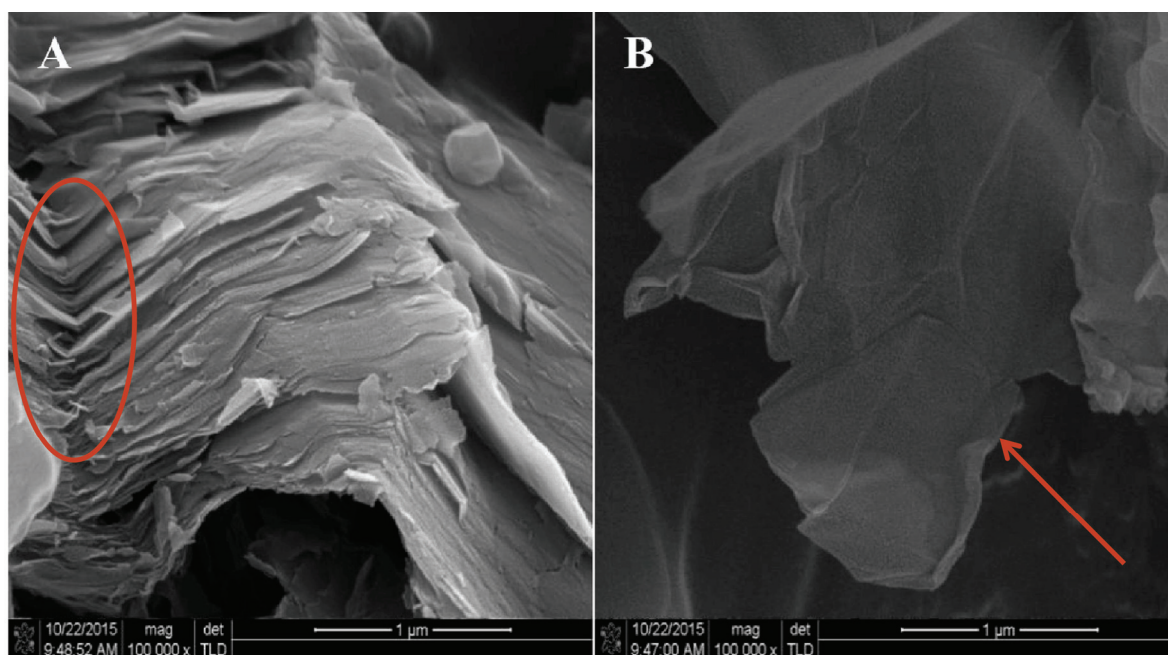

Fig. 1. SEM images of Graphite (A) and GO (B)
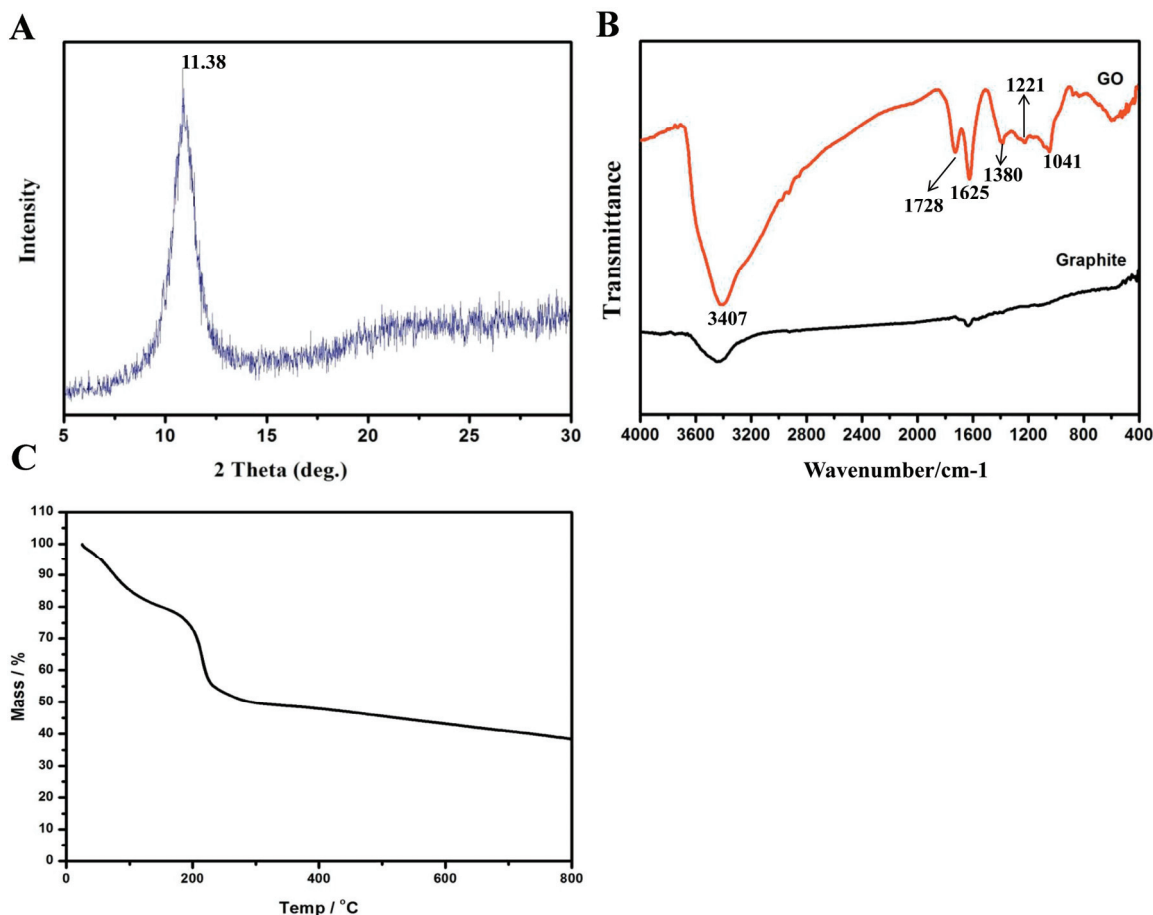
A

B

C

Fig. 2. (A) XRD patterns showing the phase of the GO, (B) FTIR spectra
of pure Graphite and GO, (C) TGA curves of GO

to form hydrogen bonds with water molecules. The results show that GO has good hydrophilicity and dispersion.

Thermal stability

As can be seen from Fig. 2C, the thermal cracking of GO was divided into two stages. Quality loss within 0~100 °C was mainly caused by evaporation of the water molecules in graphene oxide. The main reason of quality loss between 160~280 °C was probably the oxygen-containing groups in GO, that had undergone thermal decomposition and generated volatile gas CO, CO_2 and water vapor. The thermal decomposition rate of GO was 62.6% at 800 °C.

3.2. Characterization of mineralized COL/*n*HA/GO composite

SEM

The COL/GO composite exhibited loose porous structures and had a smooth surface (Fig. 3A).

Compared to COL/GO composite, the mineralized COL/*n*HA/GO composite exhibited a rough surface morphology as evidenced by Fig. 3B. In the mineralized COL/*n*HA/GO composite, the *n*HA could be clearly observed to stick to the surface (Fig. 3C, D) and the pores (Fig. 3E, F). The deposition rate of *n*HA was slightly higher on the surface than on the hole wall because the surfaces of the composite were always in contact with the SBF solution. However, the *n*HA particles did not change the three-dimensional network structure of the composite. The connectivity of the holes was good and thus beneficial to the exchange of nutrients and excreted metabolites. The hole wall of the composite was rough, which was conducive for the adhesion of cells.

EDX Spectrums

The EDX analysis results are shown in Fig. 4 and Table 2 HA with calcium ion deficiency was achieved by biomimetic mineralization and its Ca/P ratio was approximately 1.5, which was closer to natural bone than that of pure HA (Ca/P = 1.67). The quality scores and atomic number of P and Ca increased in the composites

containing 4 wt. % GO, which indicated that GO promoted the biomineralization of collagen scaffolds. The probable mechanism could be a combination of GO and COL that facilitated the effective interaction of Ca ions with other mineral ions in the SBF solution, thereby accelerating the nucleation and deposition of HA.
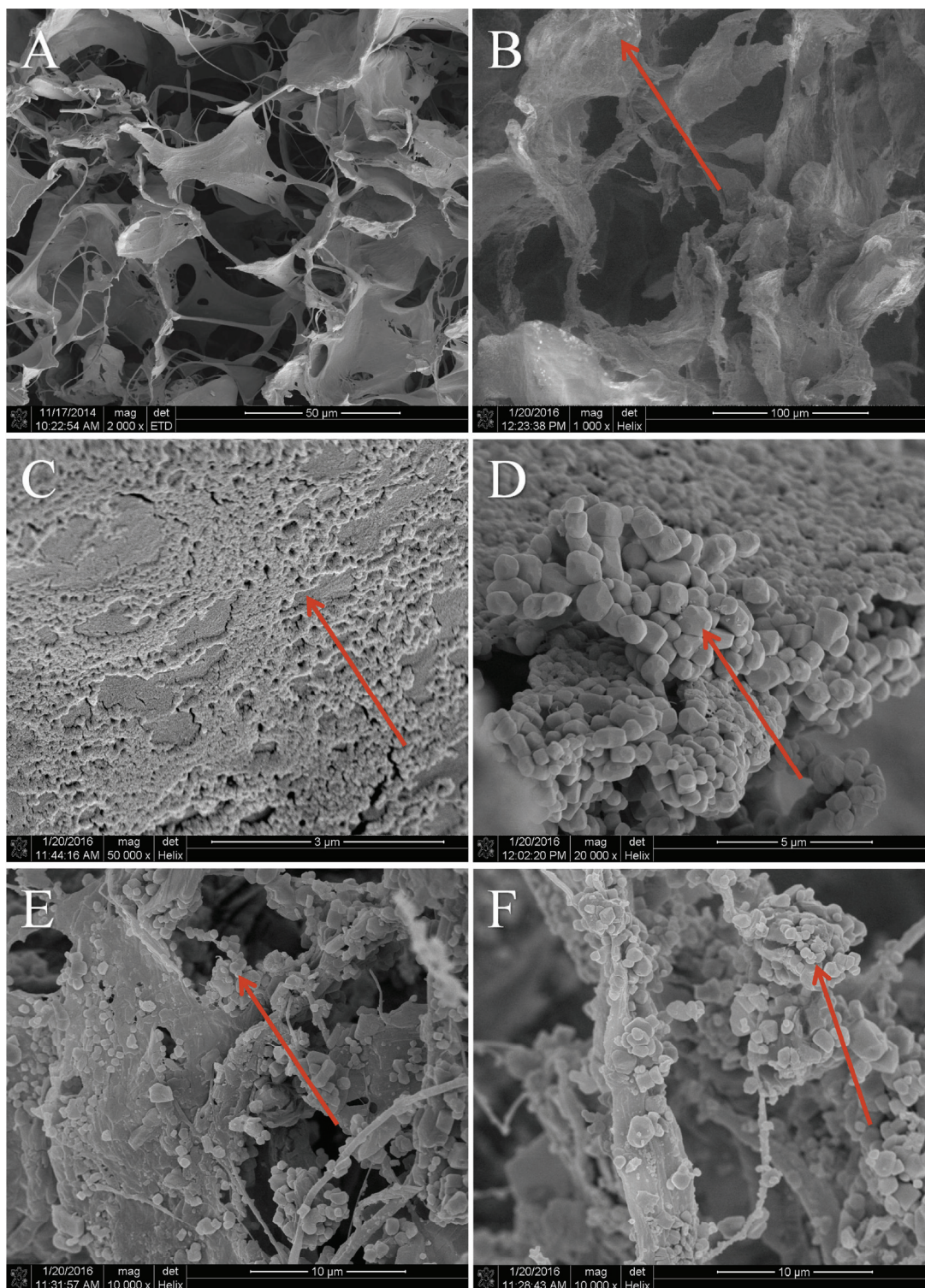

Fig. 3. (A) SEM of a section structure of COL/GO composite materials,
(B) SEM of a section structure of COL/nHA/GO composite materials,
(C, D) surface of COL/nHA/GO composite materials,
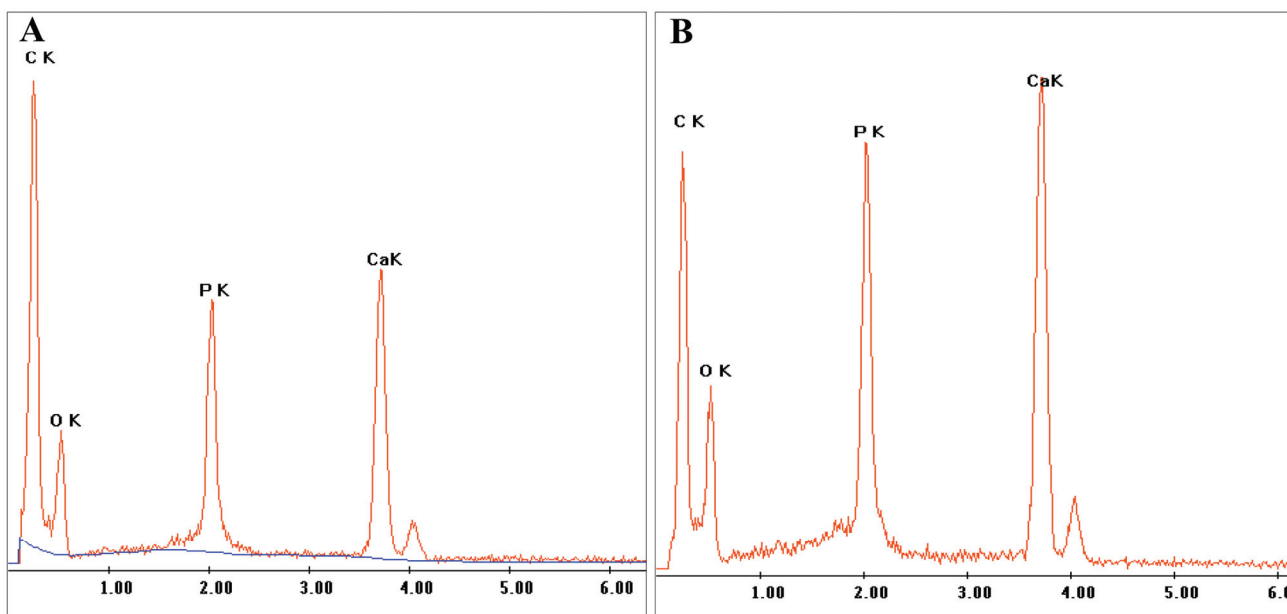(E, F) hole wall of COL/nHA/GO composite materials

Fig. 4. EDX analysis of the mineralized materials with (A) GO 1 wt. % and (B) GO 4 wt. %

Table 2. Element mass fraction
and atomic number fraction of the mineralized materials
with (A) GO 1 wt. % and (B) GO 4 wt. %

A

Elem	Wt. %	At. %
C K	18.40	35.50
O K	15.42	22.33
P K	22.92	17.15
Ca K	43.26	25.01

B

Elem	Wt. %	At. %
C K	11.48	24.42
O K	15.22	24.30
P K	24.24	20.00
Ca K	49.07	31.28

XPS spectrum

The contents of Ca and P in the mineralized composite materials were measured by XPS surface energy spectrum technology. Figure 5A shows the XPS full spectrum of the mineralized composite materials containing 1 wt. % and 4 wt. % GO. The Ca and P elements in two types of composite materials showed no significant difference in energy peak, which further confirmed the results of SEM and EDX. The result supported that the mineralization of the COL/GO composite material occurred with a certain degree of inorganic-organic hybrid. The structure and composition of the mineralized COL/HA/GO composites were similar to those of natural bone.
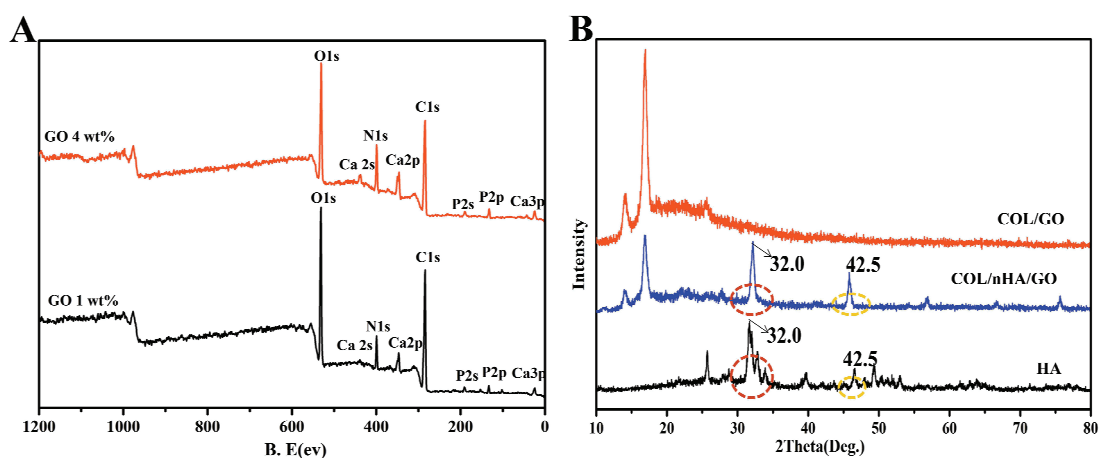

Fig. 5. (A) XPS analysis of the scaffolds after mineralization with GO 1 wt. % and GO 4 wt. %, (B) XRD patterns showing the phase of cross-linked HA and COL/GO before and after mineralization for 3 days

XRD spectrogram

The XRD spectrogram of pure HA and COL/GO composites is shown in Fig. 5B. The characteristic diffraction absorption peaks of the *n*HA crystal surface (32.0° and 46.5°) were found in the mineralized COL/*n*HA/GO composites and pure HA after mineralization for 3 days. These two absorption peaks did not appear on the surfaces of the composites that were mineralized in the non-soaked SBF solution. This finding indicates that two diffraction peaks were attributable to the nucleation of *n*HA during mineralization. In this experiment, *n*HA generation was observed in the COL/GO composites under *in situ* synthesis conditions.

3.3. Bacteriostatic test of mineralized COL/*n*HA/GO composite

The antibacterial coil method was used to measure the bacteriostasis of the mineralized COL/nHA/GO composites and the size of inhibition zone in the process of *Staphylococcus aureus* growth were used to evaluate the antimicrobial properties of the composites.

In Fig. 6, the antibacterial ring around GO powder was obvious, indicating that GO powder possesses remarkable bacteriostasis. This result is consistent with previous research results [4], [18], [31]. There was almost no inhibition zone around the pure collagen membrane. The results showed that the antibacterial properties of pure collagen were poor. Compared to the pure collagen membrane, the COL/GO composite was surrounded by an obvious bacteriostatic

ring. The average length of the bacteriostatic ring in the COL/GO composite (4 wt. % GO) was about 2 cm and in the COL/GO composite (1 wt. % GO) was about 1.6 cm. The results indicated that the antibacterial properties of collagen increased after the addition of GO and that they improved along with the increase of GO content in a certain range. The role of COL/GO composite surface in the inhibition of *Staphylococcus aureus* can be attributed to the composite material in the blocking of bacteria and nutrients or oxidative stress. Therefore, improving the surface roughness of materials can promote the inhibition of bacteria.
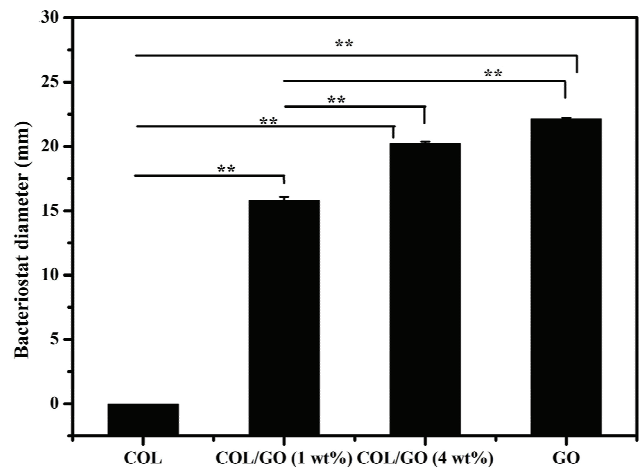

Fig. 6. Inhibition zone of different composites

3.4. Cell viability and proliferation

The viability and morphology of osteoblasts in the COL/nHA/GO composite materials were evaluated via AO/EB staining. As shown in Fig. 7(A), viable
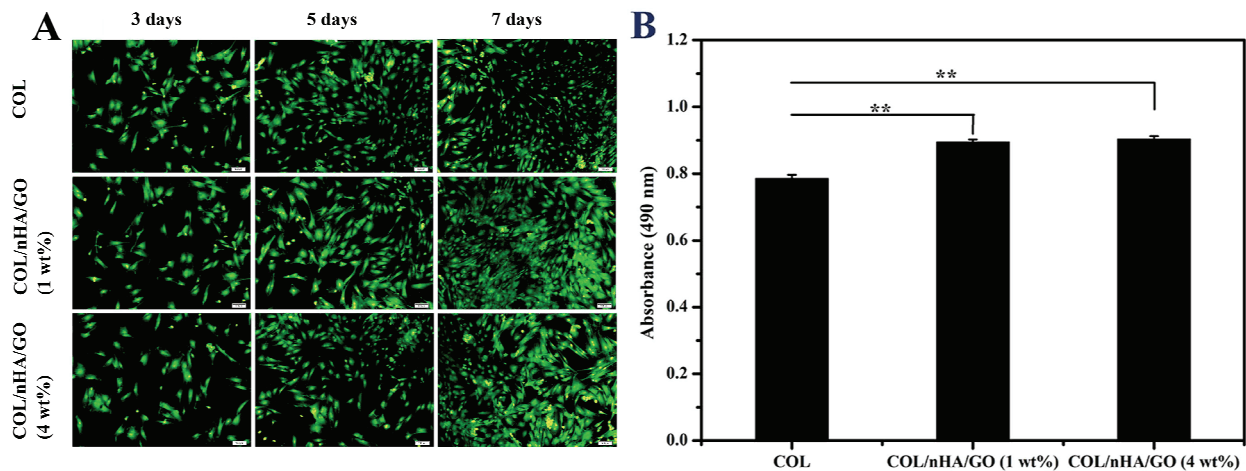

Fig. 7. (A) AO/EB staining of osteoblasts in the leach liquor of COL, COL/*n*HA/GO (1 wt. %) and COL/*n*HA/GO (4 wt. %) composite material after 3, 5 and 7 days of culture, (B) Proliferation of osteoblasts cultured on COL, COL/*n*HA/GO (1 wt. %) and COLl/*n*HA/GO (4 wt. %) composite materials after 7 days of culture

cells exhibited a bright green and apoptotic cells appeared red orange. A large number of bright green dots were observed after 3-, 5- and 7-days culture. The result indicated that osteoblasts have better activity in COL/*n*HA/GO composite. The COL/*n*HA/GO composite also provided suitable and favorable physiological environment for cell attachment.

The growth and proliferation of osteoblasts in the leach liquor of COL/*n*HA/GO composite material are shown in Fig. 7B. The osteoblasts showed good proliferation capability in three groups. Compared to the situation in the COL control group, the absorbance of osteoblasts on the composites (1 wt. % and 4 wt. % GO) was significantly increased. No statistically significant difference was observed between the COL/*n*HA/GO 1 wt. % and COL/*n*HA/GO 4 wt. % groups ($p > 0.05$). The mineralized COL/*n*HA/GO composites had good biocompatibility.

4. Discussion

Biomimetic mineralization is conducted to prepare scaffold materials for bone tissue engineering. Biomimetic mineralized scaffolds have been used for bone injury treatment in the past several decades. In this study, COL/nHA/GO composite materials were prepared through the SBF method with COL/GO as a matrix template.

SEM demonstrated that *n*HA particles appeared on the surface and hole wall of the composite materials. Furthermore, after mineralization, the *n*HA particles preserved the structural and improved biomechanical integrity of the COL/*n*HA/GO composite. It happened because biomimetic mineralization can synthesize mineral materials that have similar structures and properties to natural bone. XPS, EDX spectra, and XRD patterns exhibited significant Ca and P peaks. The results showed that the prepared composite was mineralized COL/*n*HA/GO. Antibacterial assay of the composites showed an inhibiting effect on *S. aureus* bacterial growth. Within a certain range, the bacteriostatic properties of the mineralized COL/*n*HA/GO composite improved with the increase of GO content. This is consistent with the previous results, which found that GO composite has good bacteriostatic properties [4], [18], [31]. The proliferation of osteoblasts in the biomimetic mineralized composite materials was obtained with the MTT method. The materials after mineralization exhibited no cytotoxic effect on osteoblasts and demonstrated remarkable biocompatibility. It is related to the good biocompatibility of COL and GO.

Because GO has no significant effect on cell proliferation, there was no significant difference in cell proliferation and activity among different concentrations of GO (1 wt. % and 4 wt. %). Composite materials can overcome the disadvantages of a single material, so the result of AO/EB staining indicated that osteoblasts has a better activity in COL/*n*HA/GO composite than in pure COL scaffolds. These results showed that the composition of the scaffolds provided a suitable and favorable physiological environment for cell attachment and could become a promising candidate for bone tissue engineering.

5. Conclusion

In this work, the single lamellar structure of GO powder was prepared via an improved Hummers' method. Then, COL/GO composites were immersed in SBF (1.5×SBF) for biomimetic mineralization to obtain COL/*n*HA/GO composite materials. SEM, XPS, EDX spectra, and XRD of the mineralized COL/*n*HA/GO composites were examined. The results showed that *n*HA was synthetized *in situ* in the COL/GO composites. The antibacterial properties of collagen increased after the addition of GO. The results of MTT and AO/EB showed that the mineralized COL/*n*HA/GO composites exhibited no cytotoxic effect on osteoblasts and had good cellular activity. In summary, the COL/*n*HA/GO composite materials exhibited remarkable physical and chemical properties and biocompatibility, and had the potential to be used in bone repair tissue engineering.

Acknowledgements

References

[1] ALVES N.M., LEONOR I.B., AZEVEDO H.S., REIS R.L., MANO J.F., *Designing Biomaterials Based on Biomineralization of Bone*, J. Mater. Chem., 2010, 20(15), 2911–2921.

[2] COELHO P.G., TAKAYAMA T., YOO D., JIMBO R., *Nanometer-scale features on micrometer-scale surface texturing: A bone histological, gene expression, and nanomechanical study*, Bone, 2014, 65(4), 25–32.

[3] DREYER D.R., PARK S., BIELAWSKI C.W., *The chemistry of graphene oxide*, Chem. Soc. Rev., 2010, 39(1), 228–240.

[4] DREYER D.R., PARK S., BIELAWSKI C.W., DIMIEV A.M., *The chemistry of graphene oxide*, Chem. Soc. Rev., 2010, 39(1), 228–240.

[5] ENGELHARDT E.M., MICOL L.A., HOUIS S., WURM F.M., HILBORN J., HUBBELL J.A., FREY P., *A collagen-poly(lactic acid-co-ε-caprolactone) hybrid scaffold for bladder tissue regeneration*, Biomaterials, 2011, 32(16), 3969–3976.

[6] FAN H., WANG L., ZHAO K., LI N., SHI Z.J., GE Z.G., JIN Z.X., *Fabrication, Mechanical Properties, and Biocompatibility of Graphene-Reinforced Chitosan Composites*, Biomacromolecules, 2010, 11(9), 2345–2351.

[7] HUMMERS W.S., OFFEMAN R.E., *Preparation of graphitic oxide-journal of the american chemical society (ACS publications)*, Am. Chem. Soc., 2015, 9, 8165–8175.

[8] HU W., PENG C., LUO W., LV M., LI X.M., LI D., HUANG Q., FAN C.H., *Graphene-based antibacterial paper*, Acs. Nano., 2010, 4(7), 4317–4323.

[9] JOHN C., *The structure and mechanics of bone*, J. Mater. Sci., 2012, 47(1), 41–54.

[10] KIM H., CHE L., HA Y., *Mechanically-reinforced electrospun composite silk fibroin nanofibers containing hydroxyapatite nanoparticles*, Mater Sci. Eng. C., 2014, 40, 324–335.

[11] KOLK A., HANDSCHEL J., DRESCHER W., ROTHAMEL D., KLOSS F., BLESSMANN M., HEILAND M., WOLFF K.D., SMEETS R., *Current trends and future perspectives of bone substitute materials: from space holders to innovative biomaterials*, J. Cranio. Maxill. Surg., 2012, 40(8), 706–718.

[12] LI N., WANG Z.Y., ZHAO Z.Y., SHI Z.J., GU Z.N., XU S.K., *Large scale synthesis of N-doped multi-layered grapheme sheets by simple arc-discharge method*, Carbon, 2010, 48, 255–259.

[13] LIANG J., HUANG Y., ZHANG L., WANG Y., MA Y.F., GUO T.Y., CHEN Y.S., *Molecular-Level Dispersion of Graphene into Poly(vinyl alcohol) and Effective Reinforcement of their Nanocomposites*, Adv. Funct. Mater, 2009, 19(14), 2297–2302.

[14] LUO Y., SHEN H., FANG Y., CAO Y.H., HUANG J., ZHANG M.X., DAI J.W., SHI X.Y., ZHANG Z.J., *Enhanced proliferation and osteogenic differentiation of mesenchymal stem cells on graphene oxide-incorporated electrospun poly(lactic-co-glycolic acid) nanofibrous mats*, Acs. Appl. Mater Inter., 2015, 7(11), 6331–6339.

[15] MOROZOWICH N.L., NICHOL J.L., ALLCOCK H.R., *Investigation of Apatite Mineralization on Antioxidant Polyphosphazenes for Bone Tissue Engineering*, Chem. Mater, 2012, 24(17), 3500–3509.

[16] MAUFFREY C., BARLOW B.T., SMITH W., *Management of segmental bone defects*, J. Am. Acad. Orthop. Sur., 2015, 23(3), 143–153.

[17] MIN L., QING H., FAN C.H., FANG H.P., *Destructive extraction of phospholipids from Escherichia coli membranes by graphene nanosheets*, Nat. NanoTechnol., 2013, 8(8), 594–601.

[18] OYER A.J., CARRILLO J.Y., HIRE C.C., SCHNIEPP H.C., ASANDEI A.D., DOBRYNIN A.V., ADAMSON D.H., *Stabilization of graphene sheets by a structured benzene/hexafluorobenzene mixed solvent*, J. Am. Chem. Soc., 2012, 134(11), 5018–5021.

[19] PANDA N., BISSOYI A., PRAMANIK K., BISWASET A., *Development of novel electrospun nanofibrous scaffold from P. ricini and A. mylitta silk fibroin blend with improved surface and biological properties*, Mater Sci. Eng. C., 2015, 48, 521–532.

[20] ROCHEFORT G.Y., PALLU S., BENHAMOU C.L., *Osteocyte: the unrecognized side of bone tissue*, Osteoporosis Int., 2010, 21(9), 1457–1469.

[21] SOWMYA S., BUMGARDENER J.D., CHENNAZHI K.P., NAIRET S.V., *Role of nanostructured biopolymers and bioceramics in enamel-dentin and periodontal tissue regeneration*, Prog. Polym. Sci., 2013, 38(10–11), 1748–1772.

[22] SHRIVATS A.R., MCDERMOTT M.C., HOLLINGER J.O., *Bone tissue engineering: state of the union*, Drug. Discov. Today, 2014, 19(6), 781–786.

[23] SUK J.W., PINER R.D., AN J., RUOFF R.S., *Mechanical Properties of Monolayer Graphene Oxide*. Acs. Nano., 2010, 4(11), 6557–6564.

[24] SHEN Y., YANG S.Z., LIU J.L., XU H.Z., SHI Z.L., LIN Z.Q., YING X.Z., GUO P., LIN T., YAN S.G., *Engineering Scaffolds Integrated with Calcium Sulfate and Oyster Shell for Enhanced Bone Tissue Regeneration*, Acs. Appl. Mater Inter., 2014, 6(15), 12177–12188.

[25] TASLI P.N., AYDIN S., YALVAC M.E., ŞAHIN F., *Bmp 2 and Bmp 7 Induce Odonto-And Osteogenesis of Human Tooth Germ Stem Cells*, Appl. Biochem. Biotech., 2014, 172(6), 3016–3025.

[26] WANG X., GAN H., SUN T., *Chiral Design for Polymeric Biointerface: The Influence of Surface Chirality on Protein Adsorption*, Adv. Funct. Mater., 2011, 21(17), 3276–3281.

[27] WANG K., RUAN J., SONG H., ZHANG J.L., YAN W., GUO S.W., *Biocompatibility of graphene oxide*, Nanoscale Res. Lett., 2011, 6(1), 1–8.

[28] WANG J.H., YANG Q., CHENG N.M., TAO X.J., ZHANG Z.Z., SUN X.M., ZHANG Q.Q., *Collagen/silk fibroin composite scaffold incorporated with PLGA microsphere for cartilage repair*, Mater Sci. Eng. C Mater Biol. Appl., 2016, 61, 705–711.

[29] XIA Z.M., WEI W., WURM F.M., HILBORN J., HUBBELL J.A., FREY P., *Biomimetic fabrication of collagen-apatite scaffolds for bone tissue regeneration*, J. Biomater. Tissue Eng., 2013, 3(4), 369–384.

[30] YANG G.H., KIM M., KIM G., *A hybrid PCL/collagen scaffold consisting of solid freeform-fabricated struts and EHD-direct-jetprocessed fibrous threads for tissue regeneration*, J. Colloid Interface Sci., 2015, 450, 159–167.

[31] Y, T., *Destructive extraction of phospholipids from Escherichia coli membranes by graphene nanosheets*, Nature Nanotechnology, 2013, 8(8), 594–601.

[32] ZHANG X., YIN J., PENG C., HU W.Q., ZHU Z.Y. W. X., FAN C.H., HUANG Q., *Distribution and biocompatibility studies of graphene oxide in mice after intravenous administration*, Carbon, 2011, 49(3), 986–995.